A Fast Bolometer for the WVII-AS Stellarator

H. J. Jäckel, G. Kühner, J. Perchermeier

IPP 2/291 April 1988

MAX-PLANCK-INSTITUT FÜR PLASMAPHYSIK

8046 GARCHING BEI MÜNCHEN

MAX-PLANCK-INSTITUT FÜR PLASMAPHYSIK

GARCHING BEI MÜNCHEN

A Fast Bolometer for the WVII-AS Stellarator

H. J. Jäckel, G. Kühner, J. Perchermeier

IPP 2/291 April 1988

Die nachstehende Arbeit wurde im Rahmen des Vertrages zwischen dem Max-Planck-Institut für Plasmaphysik und der Europäischen Atomgemeinschaft über die Zusammenarbeit auf dem Gebiete der Plasmaphysik durchgeführt.

Abstract

A fast germanium bolometer for plasma diagnostics in the WVII-AS advanced stellarator is described. A stainless-steel foil is used as absorber, and germanium as thermally sensitive material. Short response time and high sensitivity of the bolometer where achieved using a $1.6\,\mu m$ MgO layer as insulation between the germanium and the SS foil and by doping the germanium with oxygen, respectively. An overall heat capacity $C_{bol} = 2.1\ mJ/K$ and a temperature coefficient α of the germanium of $\alpha \equiv \frac{\Delta R/R}{\Delta T} \simeq 4\ \%/K$ were thus obtained. The thermal response time is $\tau_r \approx 10\ \mu s$ and the decay time $\tau_d \approx 1\ s$. Two 30-channel cameras for diagnostics in WVII-AS are to be equipped with the bolometers.

Introduction

In plasma physics experiments a non-negligible amount of heating power is dissipated by radiation[1] due to the inevitable presence of impurities released from the wall of the vacuum vessel and from the limiter(s) and diffusing through seals and pumping systems. In addition, highly stripped impurity ions in the plasma center lead to proton (deuteron) depletion. Great efforts are being made in experiments now running to identify the individual impurity species and study their penetration mechanism into the confinement region in order to develop schemes for reducing the impurity content[2,3,4]. A knowledge of the radial distribution and time evolution of the radiation is necessary for studying transport and energy balances.

The energy $E_{h\nu}$ of the plasma radiation ranges from a few eV to several keV, depending upon the electron temperature T_e, the radial position of the emitting volume and the impurity species. Various detectors have been developed for this energy range, making use of the internal photo effect (semiconductor diodes), photo effect and secondary electron emission (photo multipliers) or simply the heating effect of absorbed radiation (bolometers). Owing to their principle of operation, bolometers measure energy integrated and can easily be tailored to make them sensitive in the energy range of interest.

Bolometers usually consist of a metallic absorber foil which is exposed to the radiation source. The absorbed radiation power is derived from the change of the resistance of the absorber foil or of an additional resistive layer which is in good thermal contact with the absorber. The lower $E_{h\nu}^{low}$ and the upper energy threshold $E_{h\nu}^{up}$ are given by the onset of reflection from and transmission through the absorber foil, respectively. To gain high sensitivity the heat capacity of the bolometer has to be low, which can be achieved by selecting suitable materials and/or reducing the overall thickness. This affects, on the other hand, the upper energy threshold $E_{h\nu}^{up}$, and so a compromise has to be made between the sensitivity and energy detection range $\Delta E_{h\nu}$. For bolometers used in fusion research the detection range is typically $5 \leq E_{h\nu}[eV] \leq 10000$[5,6].

To measure the radial distribution of the plasma emissivity, bolometer arrays are frequently arranged in a pinhole camera with a common slit parallel to the plasma axis, giving typical radial resolutions of $\frac{\Delta r}{a} \approx 0.1$.

The WVII-AS stellarator experiment will feature an improved version of the bolometer used in its predecessor WVII-A, which has higher sensitivity and refined technical layout to reduce electrical distortion. The bolometer utilizes the high temperature coefficient of the electrical resistance of amorphous germanium, which can fairly easily be manipulated in certain limits by proper doping. Two 30-channel pinhole cameras are to be equipped with these bolometers.

Construction of the Germanium Bolometer

The germanium bolometers[7] are produced at IPP by vapour deposition. A carefully cleaned stainless-steel foil is stretched smooth in a circular frame. Different layers are subsequently vapour-deposited on this substrate by using circular masks with gradually decreasing diameter:

1. Aluminum (thickness: 1000 $\AA$), to improve adhesion.
2. Magnesium oxide (15,000 $\AA$), as insulation layer.
3. Germanium (15,000 $\AA$), doped with oxygen, as thermometer material.
4. Gold (5,000 $\AA$), using a grid mask, to form suitable electrodes for measuring the resistance of the germanium layer.

The temperature of the substrate is carefully adjusted and controlled for the subsequent evaporation steps. Figure 1 shows a schematical cross section of a bolometer.

Although the MgO layer is prepared sandwich-like in several steps, it occasionally tends to show pinholes, which electrically shunt the insulation layer when the germanium is deposited. By carefully applying a capacitor discharge ($\sim 1\mu F \times 20V$) between the germanium layer and the SS substrate, these defects can be cured in many cases. Typical values for the insulation resistance achieved in the MgO-layer are $\approx 1\,G\Omega$ at $10\,V$.

Bolometers with layers of plain germanium initially used, showed but a relatively small temperature coefficient $\alpha = \frac{\Delta R/R}{\Delta T} \lesssim 2\%/K$. Depositing the germanium in the presence of some oxygen in the recipient yielded higher α-values. In effect, doping of the amorphous germanium with oxygen causes a change of the energy distribution of the density of states and eventually a beneficial increase of α. Values of the temperature coefficient of up to $\alpha \approx 5\ \%/K$ could thus be obtained. Unfortunately the conductivity drastically drops, probably owing to increasing oxidation of the germanium. A compromise has to be made between a suitable bolometer resistance R_{bol} and a slightly reduced temperature coefficient of the resistance. Typical values of bolometers now being produced are $\alpha \approx 4.1\ \%/K$ and $R_{bol} \approx 15\ k\Omega$ at room temperature.

The oxygen partial pressure can be determined, by using the optical transmission properties of the germanium layer in the visible and near IR ranges, which sensitively depend upon the oxygen content. Samples on glass substrates are prepared prior to deposition on the bolometer. Their transmission curves are compared with a master curve once worked out, and the oxygen pressure is appropriately adjusted, to fit the transmission curve of probes to the master curve.

Figure 2 shows how the onset of the optical transmission (10 %-value) of the germanium is correlated to the resistance $R(20°C)$ and the temperature coefficient α. Envisaged values are $R(20°C) \approx 15\ k\Omega$ and $\alpha \approx 4\%/K$, these corresponding to onset of the transmission at 1185 nm and an oxygen concentration of the germanium of about 3 $at\%$.

Calibration of the Bolometer

The conductivity σ of amorphous germanium can be described in a fairly wide temperature range by

$$\sigma(T) = \sigma_0 \cdot exp\left(-\frac{E_a}{kT}\right) , \tag{1}$$

where E_a varies from ~ 0.1 to ~ 1.0 , or, in terms of R,

$$R(T) = R_0 \cdot exp\left(\frac{E_a}{kT}\right) . \tag{1'}$$

The temperature rise of the bolometer in one plasma discharge is only a few tenths of C for collimated ones and a few times ten C for uncollimated ("2π") bolometers. For the sake of simplicity in the data analysis, the temperature response of the germanium layer in the small temperature ranges occurring can thus be approximated by

$$R(T) = R_0 \cdot exp\,(-\alpha T) \tag{2},$$

where R_0 is the germanium resistance at a fixed temperature, normally 0 C, and α is the temperature coefficient of the resistance. R_0 and α have to be individually measured for each bolometer. Figure 3 shows a typical calibration curve, yielding $R_0 = 25.8\ k\Omega$ and $\alpha = 0.042\ K^{-1}$.

Determination of the total heat capacity C_{bol} of the bolometer, for quantitative derivation of the energy absorbed, turns out to be more delicate. Direct measurement with visible light is aggravated by the high reflectivity of the absorber foil, which makes estimation of the amount of radiation absorbed uncertain. On the other hand, calibrated light sources in the UV range, where reflection is negligible, are not available.

Calculating C_{bol} with the values for the heat capacities of the individual materials taken from the literature, yields

$$C_{bol}^{cal} = (2.1 \pm 0.2)\ \left[\frac{mJ}{K}\right] , \tag{3}$$

the error resulting mainly from uncertainties in estimating the heat capacities of the evaporated amorphous layers, which can significantly differ from the crystalline value, depending upon the density of the layer. Complementary to this, an attempt was made to measure C_{bol} direct by a electron beam technique[7], yielding

$$C_{bol}^{meas} = (2.26 \pm 0.5)\ \left[\frac{mJ}{K}\right] . \tag{4}$$

In the analysis of WVII-A plasmas the value $C_{bol} = 2.1 \frac{mJ}{K}$ was used.

Time Response of the Bolometer

Magnesium oxide is chosen for the separation layer between the SS absorber foil and the germanium because it offers a good combination of sufficiently good thermal conductivity and excellent electrical insulation capability, which allows the insulation layer to be built thin. A short perpendicular heat diffusion time $\tau_\perp$ could thus be realised. It was experimentally determined by shooting a short laser pulse at a bolometer. For a $4\,\mu m$ SS absorber a $10-90\%$ temperature rise time $\tau_r = 7\,\mu s$ was measured. For the $5\,\mu m$ SS-foil bolometer used at present $\tau_r \approx 10\,\mu s$ can be estimated by taking into account the square dependence of the diffusion time $\tau_\perp$ on thickness.

The temperature decay of the bolometer is caused by thermal conduction to the frame and by radiation cooling. Under typical operation conditions the temperature rise during one plasma discharge is small and the bolometer is run at ambient temperatures, so that the radiation cooling is negligible. The time characteristic of the temperature decay can easily be measured just by turning off a power source exposed to the bolometer. A few perpendicular heat diffusion times $\tau_\perp$ after the turn-off, the decay can be fitted fairly well by a single exponential function, yielding a decay time $\tau_d \approx 1\ s$.

Data Analysis

The following analysis uses difference equations, which appears to be more adequate in relation to the generally used digitising data acquisition. In this context the relevant time intervals Δt are considered to be predefined by the data acquisition system.

For heat pulses much shorter than the temperature decay time τ_d, the bolometer can be treated adiabatically and the deposited energy ΔE_{abs} is immediately deduced from the observed temperature rise ΔT_{ad}

$$\Delta E_{abs} = C_{bol} \cdot \Delta T_{ad}\,, \tag{5}$$

where T_{ad} denotes the adiabatic temperature, the heat losses being assumed to be zero. If one has $\Delta t_h \gtrsim \tau_d$, the loss of the bolometer during the measurement has to be taken into account. The characteristic decay of the temperature of the bolometer $T_d(t)$ is a function of time and of the initial temperature T_i

$$T_d(t) = f(T_i, t)\,. \tag{6}$$

For the calculation of the adiabatic temperature change $\Delta T_{ad}(\Delta t)$ in the time interval Δt the measured temperature rise ΔT has to be corrected by ΔT_d

$$\Delta T_{ad}(\Delta t) = \Delta T(\Delta t) + \Delta T_d(\Delta t) \tag{7}$$

with

$$\Delta T_d(\Delta t) = \frac{df(T_i, t)}{dt} \cdot \Delta t\,. \tag{8}$$

When the temperature decay can simply be described by an exponential function $f(T_i, t) = T_i \cdot exp\left(\frac{t}{\tau_d}\right)$ and if $\Delta t \ll \tau_d$, equation (8) becomes

$$\Delta T_d(\Delta t) = -\frac{\Delta T}{\tau_d} \cdot \Delta t\,. \tag{9}$$

Starting at a temperature T_0 (frame temperature), the adiabatically corrected temperature T_{ad} after the n-th time interval is

$$T_{ad}(t_n) = T(t_n) + \frac{1}{\tau_d} \sum_{j=1}^{n} \Delta t_j \cdot \Delta T_m(t_j)\,, \tag{10}$$

$$\Delta T_m(t_j) = \frac{T(t_j) + T(t_{(j-1)})}{2} - T_0\,, \tag{11}$$

$T(t_n)$ and $\Delta T_m(t_j)$ being the temperature after the n-th and the mean temperature rise after the j-th time interval, respectively. Figure 4 shows for a WVII-A discharge the measured and the adiabatically corrected temperatures of a collimated bolometer.

The mean power P_{abs} absorbed by the bolometer in the time interval Δt is defined as

$$P_{abs}(\Delta t) = C_{bol} \cdot \frac{\Delta T_{ad}}{\Delta t} \tag{12}$$

Substituting for T_{ad} from equation (10) gives

$$P_{abs}(t) = C_{bol} \cdot \frac{\Delta}{\Delta t} \left(T(t_n) + \frac{1}{\tau_d} \sum_{j=1}^{n} \Delta t_j \cdot \Delta T_m(t_j) \right) \tag{13}$$

and eventually, if the differential time interval is $\Delta t = \Delta t_j$,

$$P_{abs}(t) = C_{bol} \cdot \left(\frac{\Delta T(t_n)}{\Delta t} + \frac{T(t_n)}{\tau_d} \right)\,. \tag{14}$$

Experimental Implications

Owing to the sandwich-like construction, the bolometer has an electrical capacitance of about 5 nF. Together with the typical resistance of the germanium layer of $R_{bol} \approx 15\,k\Omega$ (at room temperature) this yields an electrical time constant $\tau_{el} \approx 100\mu s$, which is obviously much larger than the thermal time constant $\tau_{\perp}$. To assure that solely $\tau_{\perp}$ defines the time resolution of the bolometer, discharging of the inherent capacitance has to be avoided by measuring the germanium restistance at constant voltage.

In strong magnetic fields the magneto-resistance of the germanium layer has to be taken into account. Due to the ramping up of the toroidal magnetic field prior to a plasma discharge, the bolometer shows a non-negligible change of its resistance. The magnetically induced portion of the bolometer signal has to be carfully cancelled out before analysing the data. This is being done in WVII-A/WVII-AS by applying a sample-and-hold technique, which allows one to measure the resistance in the flat-top phase of the toroidal field just before the start of the discharge. This value is taken as a reference for calculating the resistance change during the plasma discharge. The quality of the suppression of magnetic contributions to the bolometer signal can easily be verified in machine runs where all magnetic fields were applied but no discharge occurs.

Using the sample-and-hold technique, solely the change of the bolometer resistance is measured, allowing high amplification of the bolometer signal. This is particularly necessary when the bolometer is strongly collimated.

The time resolution achievable in the experiment is much worse than the ideal one defined by $\tau_{\perp}$, owing to distortions by the transient magnetic fields applied. Inevitable loops in the wiring and the finite size of the bolometer cause pick-up signals and deteriorate the signal-to-noise ratio. In WVII-A the detection limit of the bolometer was $P_{bol} \approx 40\,\mu W/cm^2$, resulting in an effective time resolution $\Delta t_r \gtrsim 2ms$ (depending upon the radiation level) for a collimated bolometer with a radial resolution of $\frac{\Delta r}{a} \approx 0.1$.

Sensitivity to Neutron Fluxes

In current fusion experiments moderate neutron yields[8] of up to $10^{10}\ cm^{-2}$ per D discharge, which are generated thermally and/or during the slowing-down of fast deuterons, can be expected. In single-crystal semiconductors this would inevitably cause a severe change of the solid-state properties. In an amorphous or vitreous semiconductor, as obtained by evaporation, the conductivity mechanism is closely correlated to the density of dangling bonds, which is a few times $10^{19}\ cm^{-3}$. It can be assumed that even at the fluxes expected, neutron induced damage would not change significantly this number and the correlated conductivity properties. This was experimentally verified by exposing one bolometer in the FRM experimental

fission reactor at Garching to a total neutron dose of $2 \times 10^{16}\ cm^{-2}$. Although the total resistance R of the germanium layer was slightly changed after the irradiation, the temperature coefficient $\alpha = \frac{\Delta R/R}{\Delta T}$, from which the energy absorbed by the bolometer is derived, has remained constant within the error of measurement (~ 3 %).

Experimental Setup

At present, efforts are being made to reduce the geometric size of the bolometers in order to minimize perturbations due to transient magnetic fields. This requires finer grid masks and refined processing. This work is in progress, but in the initial experimental stage of WVII-AS the larger standard type of bolometer is to be used. Table 1 summarizes the characteristic bolometer data. Figure 5 shows the evaporated electrode structure on the rear of a standard bolometer. On both sides of the grid two small contact areas can be seen, which allow the resistance of the germanium layer to be measured. In WVII-A we successfully used as contacts pairs of gilded CuBe wires (OD 0.125 mm) pressing smoothly onto the contact areas.

To measure the radial distribution of the plasma radiation in WVII-AS, thirty bolometers are arranged in a double array (Fig. 6) within a pinhole camera. The camera, now being designed, possesses an adjustable slit and provides the possibility of inserting two different filters alternatively in the slit position. Figure 7 shows the fan of the lines of sight of one camera. Two cameras poloidally separated from each other by $\sim 75^o$ are to be installed to provide the possibility of applying tomographic analysis.

A 10-channel system (Fig. 8) already used in WVII-A can also be mounted on WVII-AS. Each bolometer of this system carries its own collimator, made from a stack of etched metal sheets, thus allowing a compact layout.

Summary

In WVII-AS germanium bolometers having high sensitivity and short response time are to be used. The processing of the bolometers has been improved to give predictable characteristics. Efforts are being made to optimize the layout to further reduce electrical and/or magnetic pick-up due to transient fields during the discharge.

Two 30-channel pinhole cameras, poloidally separated from each other by 75^0, are to be equipped with these bolometers. The cameras are now being designed with the aim to allow the slit to be adjusted and two filters to be moved alternatively into the slit position by remote handling.

Acknowledgments

The technical processing of the bolometers and all the activities necessary for contacting, wiring and mounting require great skill and dexterity. The authors would like to stress that this work could not have been done without the commitment of A. Gronmayer and they would like to thank him very much. They are further very much obliged to M. Karpfinger, who did the evaporation work.

Doping the germanium layer with oxygen, to increase the temperature coefficient α was suggested by K. Kempter from SIEMENS-Forschungslabor, Munich. The authors would like to thank him very much for his active support and valuable advice.

Geometry:		
outer diameter	*21.5/16.5*	*mm*
inner diameter	*14.0*	*mm*
height	*4.0*	*mm*
Layer thicknesses:		
SS absorber	*5.0*	μm
MgO insulator	*1.5*	μm
Ge thermistor	*1.5*	μm
Au electrode	*0.5*	μm
Physical properties:		
resistance	$R(T = 20^oC) \approx 15$	$k\Omega$
temp. coefficient	$\alpha \equiv \frac{\Delta R/R}{\Delta T} \approx 4$	$\%/K$
heat capacity	$C_{bol} \approx 2.1$	mJ/K
thermal rise time	$\tau_r \approx 10$	μs
cooling time	$\tau_d \approx 1$	s

Table 1: Characteristic parameters of the germanium bolometers.

References

[1] H. J. Jäckel et al, 14^{th} Eur. Conf. on Contr. Fusion and Plasma Physics, Madrid (1987), II-718

[2] W. W. Engelhardt, JET-P(86)27 (1986)

[3] K. Behringer, Rev. Sci. Instrum. 57 (1986), 2000

[4] A. WVII-A Team, NI Group, Nucl. Fus. 25 (1985), 1593

[4] K. F. Mast et al, Rev. Sci. Instrum. 56 (1985), 969

[5] E. R. Müller, K. F. Mast, J. Appl. Phys. 55 (1984), 2635

[6] H. J. Jäckel et al, 23^{th} Annual Meeting of the Division of Plasma Physics of the APS, New York (1981)

[7] G.Kühner, to be published

G.Kühner, Verhandl. DPG(V1), 21 (1986) 134

[8] G. Sadler et al, 13^{th} Eur. Conf. on Contr. Fusion and Plasma Physics, Schliersee, FRG, (1986), I-105

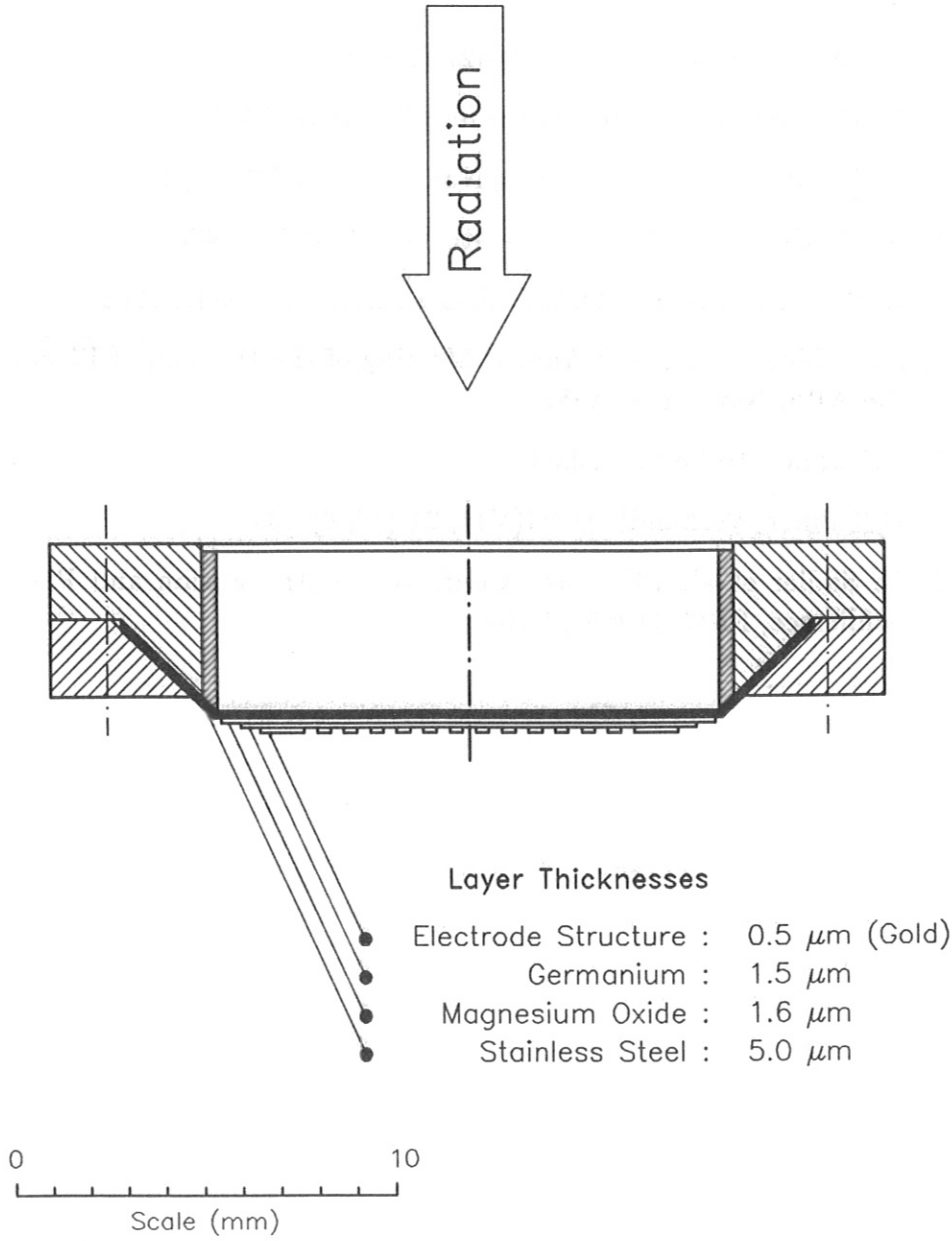

Fig. 1: Schematic cross-section of the standard type of germanium bolometer, as already used in the WVII-A experiment.

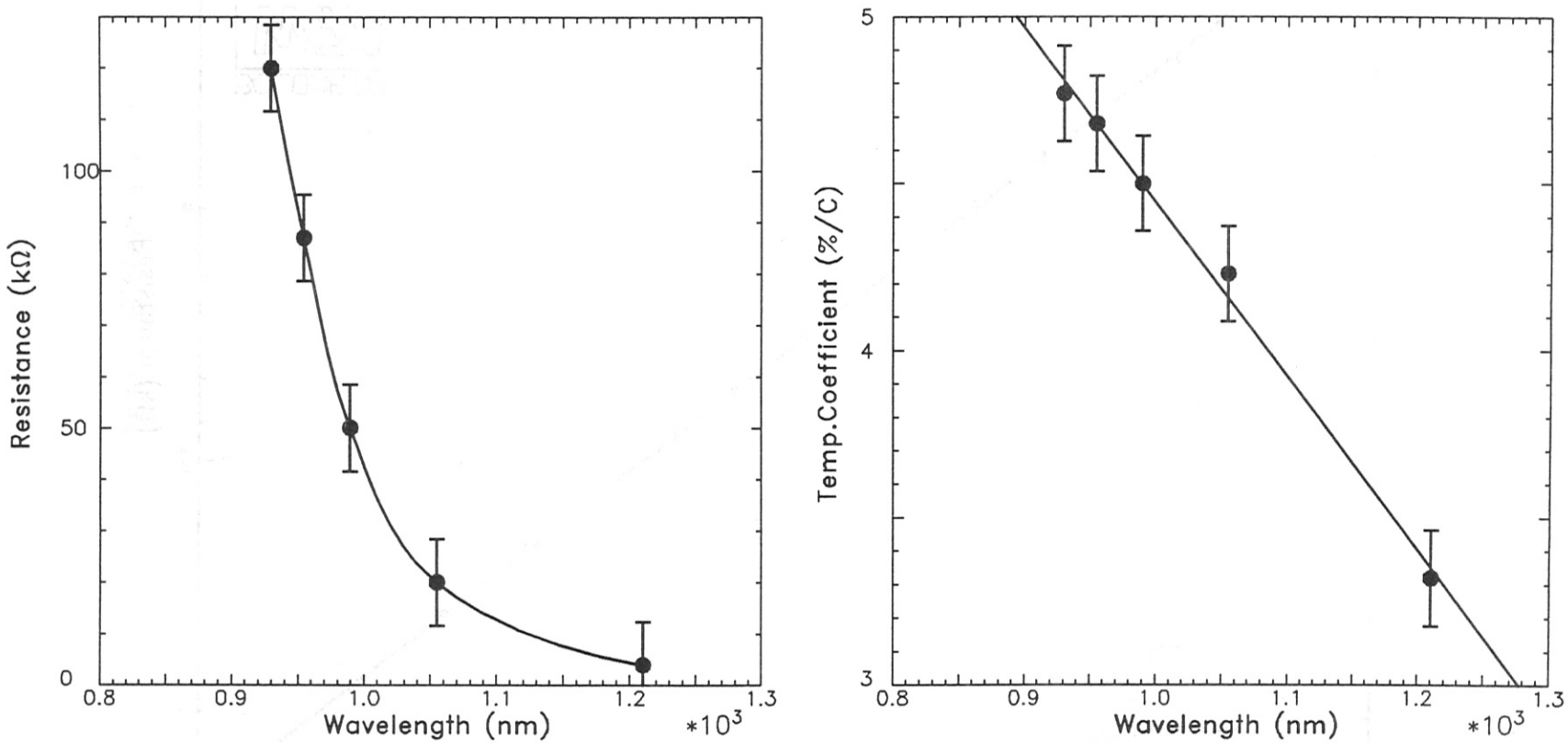

Fig. 2: The onset of the optical transmission of oxygen-doped germanium in correlation to the resistance $R(20^oC)$ (left) and the temperature coefficient α (right). For $R(20^oC) \approx 15\ k\Omega$ and $\alpha \approx 4\ \%$, the oxygen concentration is $\sim 3\ at\%$.

$$R(T) = R(T_0) \cdot exp(-\alpha T)$$

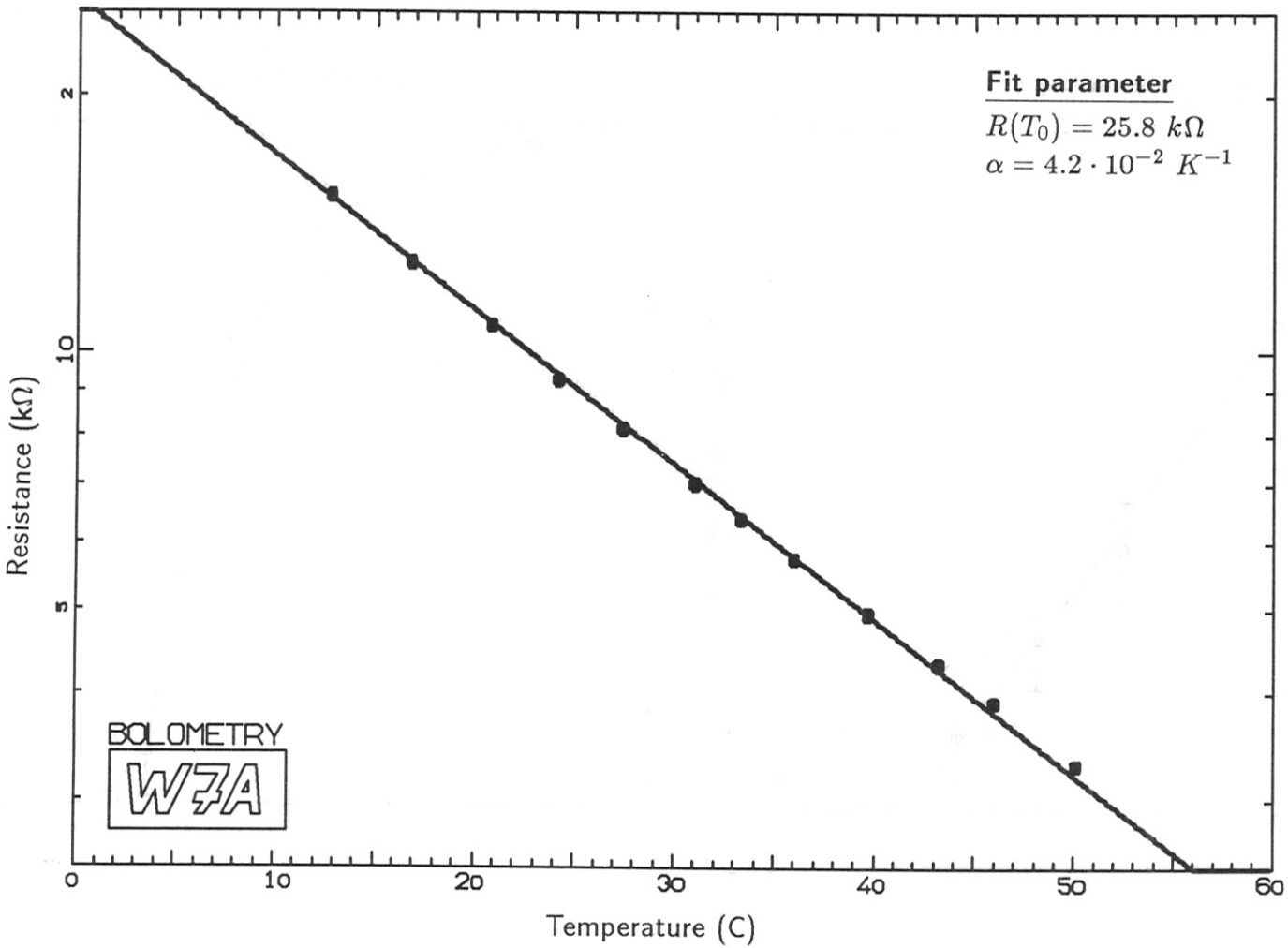

Fig. 3: Temperature characteristic $R(T)$ of the germanium resistance of a bolometer yielding $R_{bol}(20C) = 11.2\,k\Omega$ and $\alpha \equiv \frac{\Delta R/R}{\Delta T} = 4.2\,\%/K$.

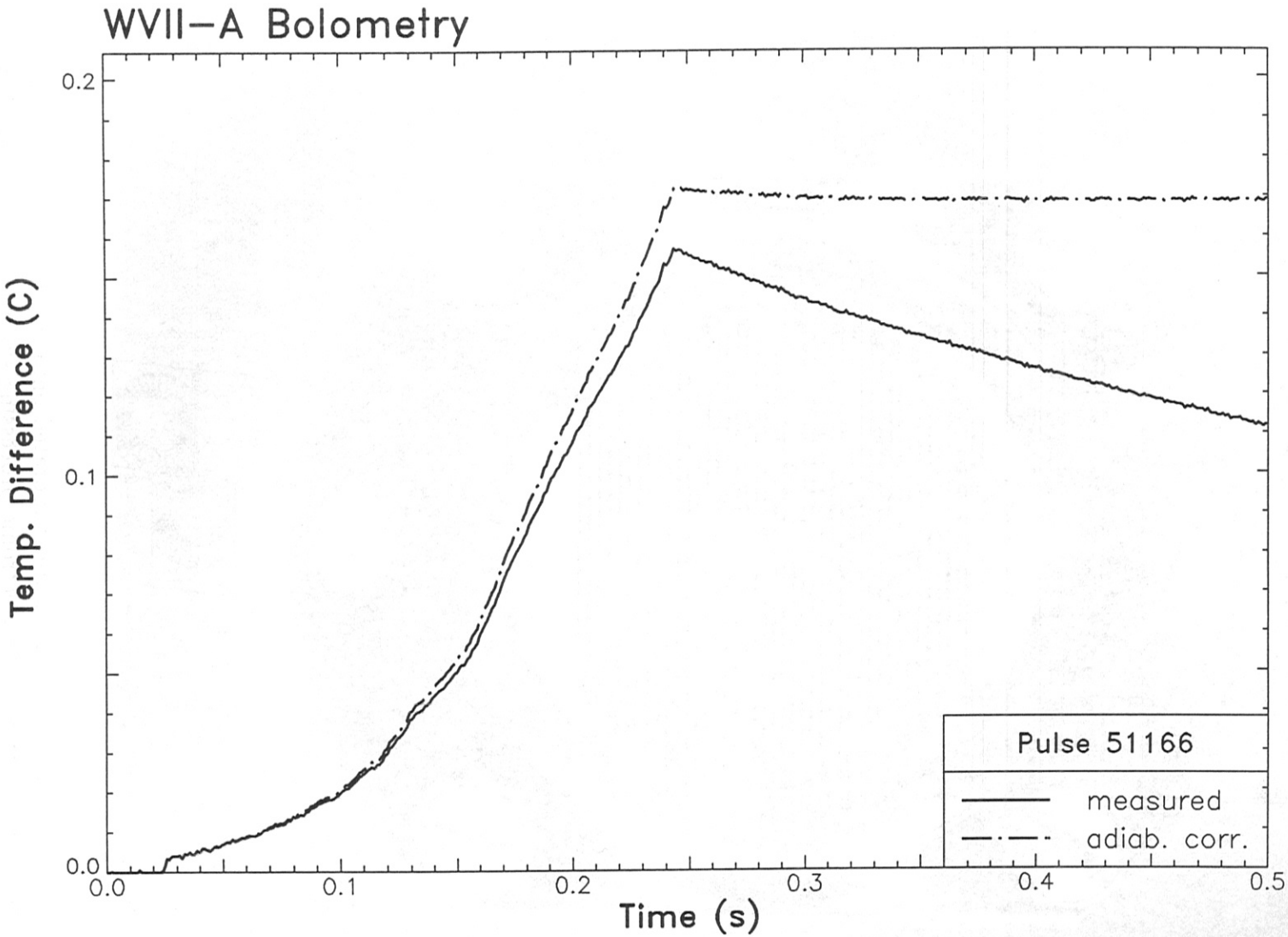

Fig. 4: Temperature rise of a bolometer during a WVII-A discharge (solid curve). The dashed-dotted curve represents the adiabatically corrected temperature T_{ad} in equation (9), assuming an exponential decay of the bolometer temperature.

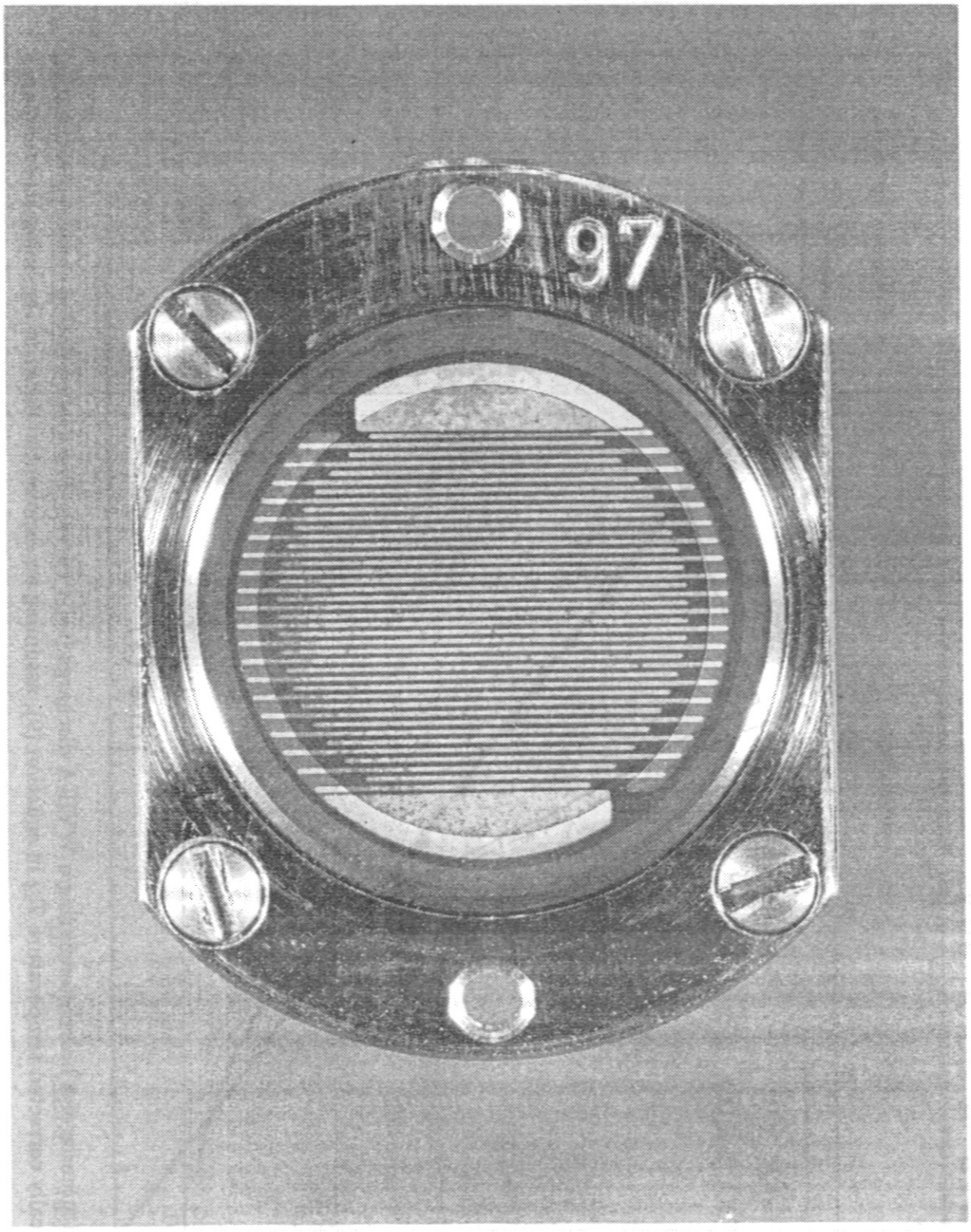

Fig. 5: Two interleaving grids of gold are evaporated onto the germanium to match the resistance better to the electronic processing system. The picture shows the rear of a bolomter. For the scale see Fig. 1.

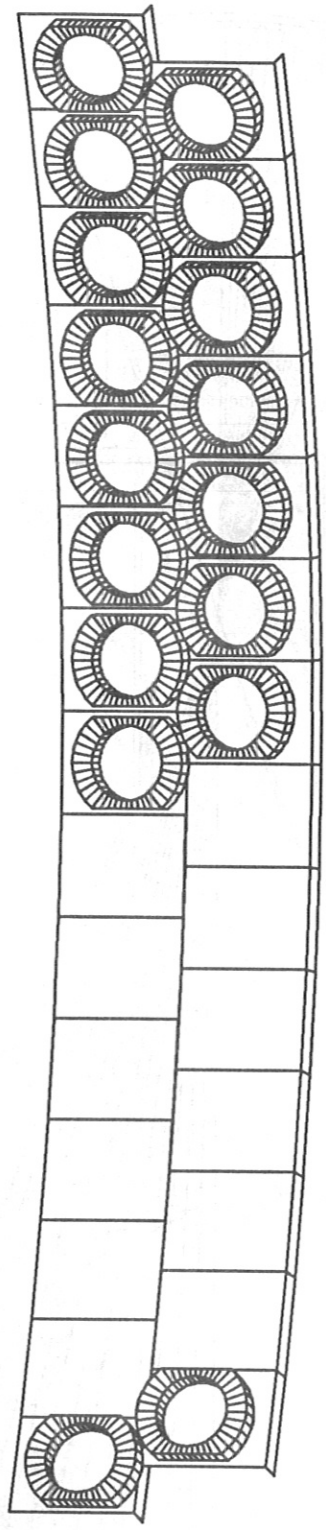

Fig. 6: Schematic sketch of the arrangement of the bolometers in the pinhole cameras. Only the upper half of the array is shown completely.

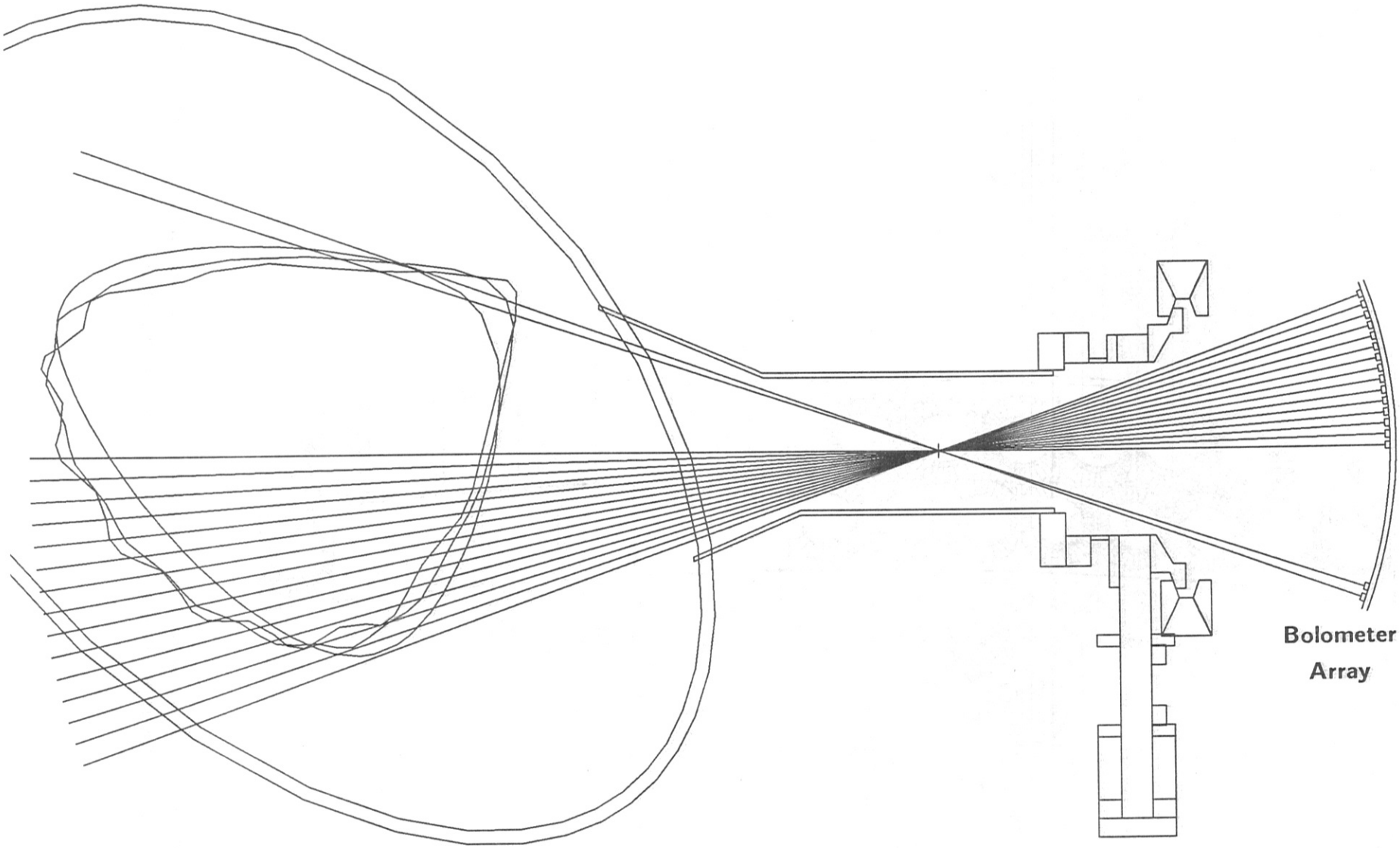

Fig. 7: Lines of sight of one bolometer camera. Only one half of the fan of chords is shown completely. The contours inside the torus cross section represent the last closed flux surfaces for $\epsilon = 0.25/0.37/0.48$.

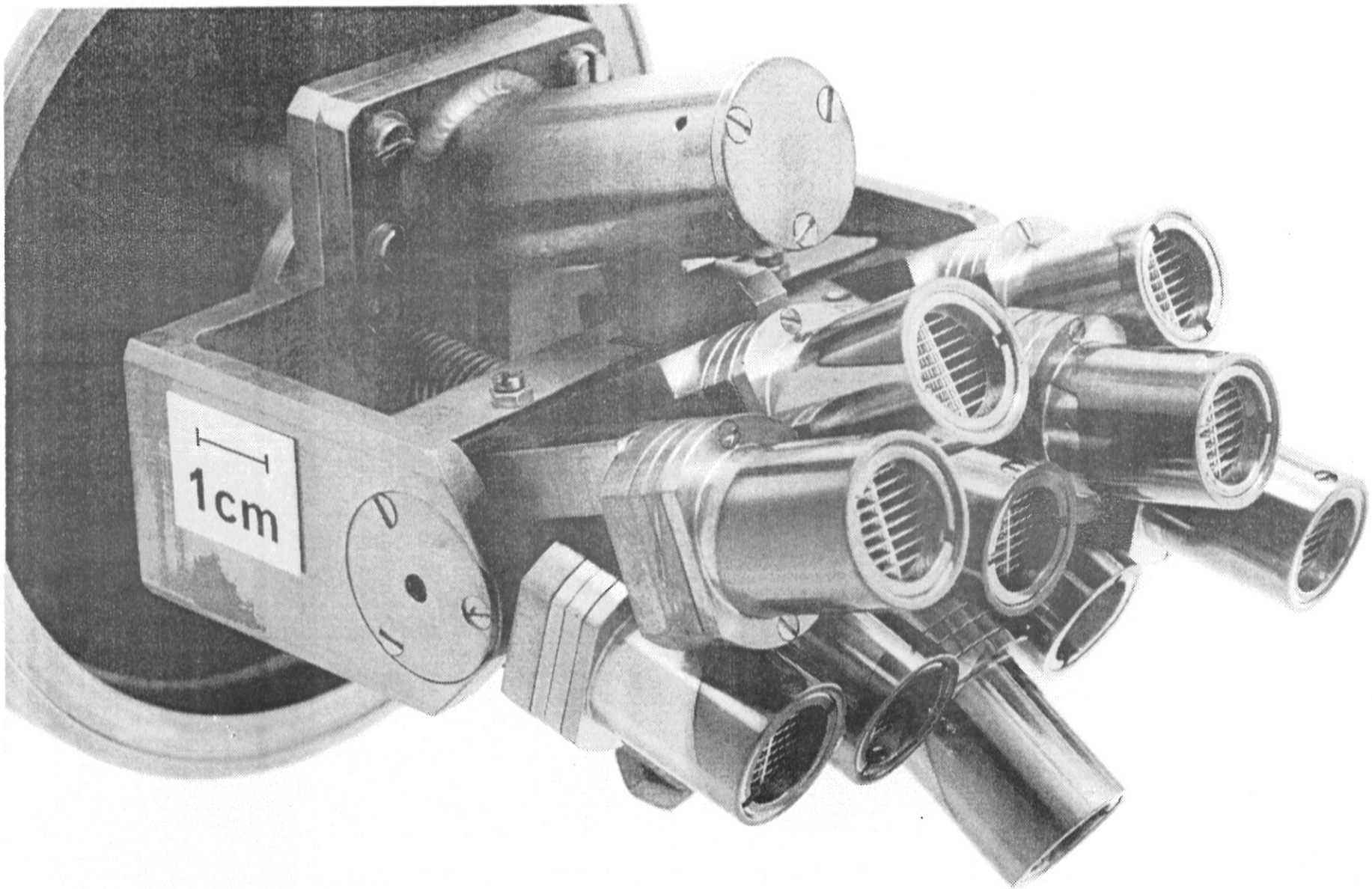

Fig. 8: Head of the 10-channel system with individual collimators for every bolometer. The collimators are made from stacks of etched metal sheets, allowing a compact layout.